Journal of Hazardous Materials 167 (2009) 418–426

Contents lists available at ScienceDirect

Journal of Hazardous Materials

journal homepage: www.elsevier.com/locate/jhazmat

Behavioral evidence of the dominant radicals and intermediates involved in Bisphenol A degradation using an efficient Co^{2+}/PMS oxidation process

Yi-Fong Huang [a], Yao-Hui Huang [a,b,*]

[a] Department of Chemical Engineering, National Cheng Kung University, Tainan City 701, Taiwan
[b] Sustainable Environment Research Center, National Cheng Kung University, Tainan City 701, Taiwan

ARTICLE INFO

Article history:
Received 12 August 2008
Received in revised form 29 October 2008
Accepted 31 December 2008
Available online 14 January 2009

Keywords:
Endocrine disrupting chemicals
Bisphenol A
Peroxymonosulfate
Radicals
Mineralization

ABSTRACT

This study investigated the degradation and mineralization of Bisphenol A (BPA) at pH 7, taken as a model compound in the presence of the trace metal-ions, Co^{2+}, and peroxymonosulfate (Oxone: PMS). We took advantage of the high oxidation–reduction potential of hydroxyl and sulfite radicals transformed from PMS as the oxidants to oxidize BPA to less complex compounds (stoichiometric ratio: $[PMS]_0/[BPA]_0 = 2$). Afterwards, the expected radicals were used to mineralize those compounds more efficiently (TOC removal ~40%) as compared to the 1% removal demonstrated in the UV/persulfate system in our previous study. To the best of our knowledge, this is the first attempt to evidence that the dominant behavior of radicals in a (bi)sulfite process is very different from that in a persulfate process. Additionally, the utilization of extremely small amounts of activator and oxidant for the complete degradation of BPA was achieved. The BPA degradation in this Co^{2+}/PMS process formulated a pseudo-first-order kinetic model well over a practicable range of 25–45 °C. The activation energy ($\Delta E = 57.6$ kJ mol^{-1}) was calculated under different conditions, and the detailed discussion indicates that the activity of BPA degradation is not obviously dependent on the PMS concentration, but rather is related to Co^{2+} dosage. Possible BPA side-chain oxidative metabolic pathways are suggested based on experimental results incorporating the evidence from EPR (electron paramagnetic resonance) and analysis from GC–MS (gas chromatography–mass spectrometry).

1. Introduction

Bisphenol A [BPA: 2,2-bis(4-hydroxyphenyl)propane] is commonly used in the synthesis of polymers including polycarbonates, epoxy resins, phenol resins, polyesters, polyacrylates, and other specialty products [1]. BPA dust (particulate) may be inadvertently released from closed systems during processing, handling, and transportation. However, the fugitive dust is controlled by workplace practices and engineering design and is not a significant contributor to environmental pollution. The relatively small amount of vapor released into the atmosphere can be rapidly degraded by sunlight. However, low levels (ppb to ppm levels) of BPA are released into effluent water, and even after biological wastewater treatment, the residuals still remain harmful to the environment and human health [2].

Recently, biphenolic compounds, including BPA, have been recognized as endocrine disrupting chemicals (EDCs) that interact with the endocrine system, interfering in the production, release, transport and metabolism of natural hormones [3]. Unfortunately, the presence of these compounds in effluents at low but environmentally relevant levels indicates that traditional technologies are not sufficiently effective for treating these compounds. Thus, it is not only necessary to assess the biodegradability or fate of BPA in the natural environment, but also to lower its toxicity. New technologies including biodegradation processes [4,5] and effective advanced oxidation processes (AOPs) [6,7] have been developed to target such compounds. However, the common drawbacks of biodegradation technologies, such as the fact that they require a long reaction time (several days to months), still remain. Even powerful AOPs do not achieve the necessary mineralization, and a large amount of sludge is discharged, creating another problem worse than the degradation itself. Moreover, AOPs such as the Fenton-type reaction are limited by low pH conditions ($pH_i < 4$) [8], and although pH can be expanded to the neutral region in the presence of iron ligands [9,10], additional amounts of additives are required, and the degradation efficiency is decreased.

As our previous work indicated [11], the novel UV-$Na_2S_2O_8/H_2O_2$-Fe(II,III) process, involving the generation of very reactive oxidizing radicals (i.e. $SO_4^{\bullet -}$ and $^{\bullet}OH$) has been sufficiently supported with regard to the mineralization of BPA as toxic organic compounds in water. Based on economic concerns, another competitive oxidation method of substitution,

* Corresponding author. Tel.: +886 6 2757575x62636; fax: +886 6 2344496.
E-mail address: yhhuang@mail.ncku.edu.tw (Y.-H. Huang).

0304-3894/$ – see front matter © 2009 Elsevier B.V. All rights reserved.
doi:10.1016/j.jhazmat.2008.12.138

cobalt/peroxymonosulfate (Co^{2+}/PMS), was employed in this study in order to avoid energy consumption (i.e. the UV source) in the UV-$Na_2S_2O_8$ processes [11]. Furthermore, as far as is known, little has been reported on the degradation of BPA in general by Co^{2+}/PMS. The use of PMS, a type of (bi)sulfite, is due to the fact that it has a higher oxidizing potential (1.82 V) than H_2O_2 (1.76 V) and intervenes in degradation processes in a more efficient way than does persulfate ($S_2O_8^{2-}$) [12,13]. Moreover, metal-ion catalyses of PMS have been reported to generate the reactive oxidative radicals, $HSO_5^{\bullet-}$, $SO_4^{\bullet-}$, and $^{\bullet}OH$, involving chain oxidative processes for the mineralization of organic pollutants [14,15].

We take advantage of the high reactivity of sulfate radicals and use PMS as the oxidant to oxidize BPA to less complex compounds (stoichiometric ratio: $[PMS]_0/[BPA]_0 = 2$). Afterwards, the expected radicals were used to mineralize those compounds by the activation of PMS with an extremely low concentration of Co^{2+} ($[Co^{2+}] = 5\ \mu g\ L^{-1}$). To the best of our knowledge, this is the first attempt to evidence that the dominant behavior of radicals in a (bi)sulfite process is very different from that in a persulfate process, and this is also the first attempt to utilize such small amounts of catalyst (i.e. activator) and oxidant for the complete degradation of BPA, rather than the large stoichiometric dosage of PMS (or persulfate) and metal-ions with the additional UV source used in other studies for the degradation of organic compounds [16,17].

Consequently, the aim of this study is to show that the use of small dosages of Co^{2+} and PMS can greatly accelerate the mineralization of BPA, which indicates a superior potential for substituting and lowering the cost of the 1st-stage of the proposed novel "UV-$Na_2S_2O_8$/H_2O_2-Fe(II, III) two-stage oxidation process" [11]. A relatively higher TOC removal of BPA in comparison with UV-$Na_2S_2O_8$ process was expected to destroy its toxicity. A significant benefit from this concept is to directly practice the treatment of BPA, even in alkaline conditions (pH ≥ 7). The powerful oxidants, which can be introduced coexistently to participate in the BPA degradation, performed as qualitatively identified $SO_3^{\bullet-}$ and $^{\bullet}OH$ radicals as indicated by EPR, and they were also particularly evidenced to demonstrate their dominance under different conditions. Furthermore, possible pathways based on the identified intermediates are suggested, and a kinetic of PMS participation in the BPA degradation is approached.

2. Experimental

2.1. Materials and methods

Bisphenol A was purchased from Showa. For reference, the chemical structure of BPA consists of two phenolic rings joined together through a bridging carbon which is displayed as the target EDC used in all trials. Potassium peroxymonosulfate (PMS: OXONE®, DuPont) was purchased from Aldrich. Cobaltous Sulfate was obtained from Showa. 5,5-dimethyl-1-pyrroline-N-oxide (DMPO) was purchased from Sigma. Other chemicals used herein, including sulfuric acid, sodium hydroxide and the phosphate buffer solution (obtained from Scharlau), were of reagent grade and were used to adjust pH. All sample solutions were prepared using deionized water from the Millipore Milli-Q system.

The metal-activation of the BPA degradation reactions in a batch photoreactor (Fig. 1) at reaction temperature was carried out. BPA reactive solutions (0.05 mM) were prepared in ~1.92 mM NaOH, ~0.92 mM phosphate buffer ($[KH_2PO_4] = 0.30$ mM and $[Na_2HPO_4] = 0.62$ mM), at pH 7. All reactions were initiated by the simultaneous addition of the estimated amounts of PMS (0.05–0.10 mM) and Co^{2+} (1.7×10^{-4}–17×10^{-4} mM, i.e. 1–10 $\mu g\ L^{-1}$) in a thermostatic water bath. The volume of all reactive solutions was 1.3 L in each trial. In order to clarify the activation ability differences from the Co(II) ions, or from bubbling with N_2(g) instead of air (i.e. O_2) to study the oxygen-dependence of the system, the comparative experiments were also initiated, such as turning on the UV light and reaching a stable emission.

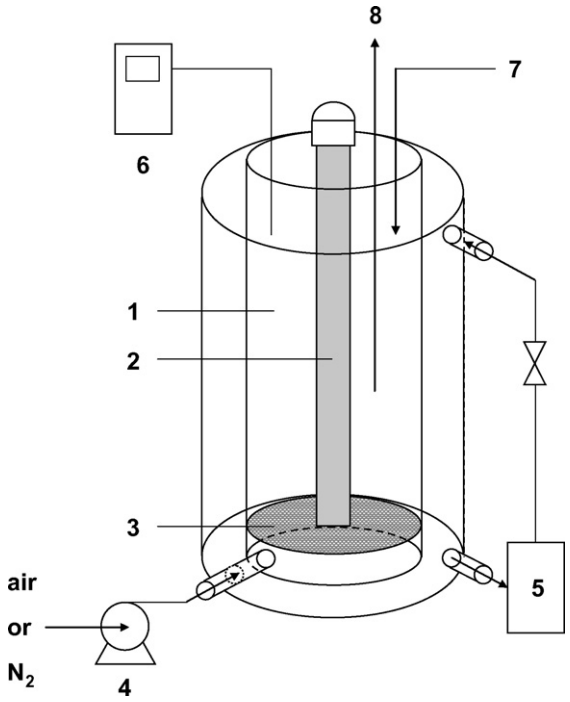

Fig. 1. Experimental equipment: (1) Photoreactor, (2) UV lamp (λ = 254 nm; background experiment), (3) Porous glass-plate, (4) Pump, (5) Thermostat, (6) Thermometer and pH meter, (7) Feeding (PMS or Co^{2+}) and (8) Sampling.

As unfavorable halogen ions such as Cl^- participate in the reaction, they simultaneously scavenge most of the radicals produced, thus generating chloride that may further transfer to Cl_2(g) as a result of the combination of two chloride atoms [18,19]. Due to the study's requirement to clarify the kinetics of the BPA/PMS oxidation system, all the reagents, including an acid source for the purpose of adjusting the pH and a Co(II,III) source required for activation, are frequently used in the sulfate form instead of the chloride form to avoid such unwanted scavengers.

2.2. Analysis

2.2.1. Analytical procedures

The residual BPA level was measured after 0.5 mL methanol was added to each sample (1 mL) to quench the radicals and thus terminate the reaction. The main absorption of BPA was at λ_{max} = 276 nm, and the removal of BPA was determined using high-performance liquid chromatography (Shimadzu 6A) with a TSK-GEL ODS-100S column (4.6 mm × 250 mm). TOC was measured using a TOC analyzer (Sievers 900 Portable). The performance of SO_4^- produced was detected using ion-exclusion chromatography with a 4.6 mm ID × 250 mm L Metrosep A SUPP 1 column (Metrohm, USA), which was not interfered with by the residual oxidants (i.e. PMS) during the reaction period. Using the atomic absorption analysis, almost no Co(II, III) ion residuals were found during the degradation of BPA in all of the oxidation processes due to the use of such extremely few amount of $[Co^{2+}]_0$.

2.2.2. UV–vis spectroscopy

UV–vis spectra were obtained using a Hewlett-Packard 8453 diode array spectrophotometer (Agilent). The decline of Co(II) species influenced by PMS was evaluated spectrophotometrically

at λ = 190–1100 nm as a background experiment (Fig. 4a and b). By deducting a background value from Fig. 4a and b, all BPA samples in the oxidation processes were analyzed immediately after sampling so as to prevent further reactions.

2.2.3. EPR measurements

An electron paramagnetic resonance spectrometer (EPR) from Bruker (model EMX-10; X-Band; 9 GHz) was used to detect whether the free radicals, $SO_4^{\bullet -}$ or $SO_3^{\bullet -}$ or $^{\bullet}OH$, were produced during the activation of PMS and with the degradation of BPA. DMPO (~0.07 M) was used as the radical spin-trapping reagent, while the EPR was operated under the following conditions: the center field = 3355 G, the sweep width = 100 G, the microwave frequency = 9.4 GHz, and the power setting = 20 mW. Samples were 20-multiple concentrated under the same conditions as all of the experimental trials in order to amplify the signal-to-noise ratio (SNR) for high resolution of the EPR spectra.

2.2.4. GC/MS identification

Organic-soluble components, indicating intermediates, were 40-multiple extracted with 2.5 mL of dichloromethane. For experiments using PMS, samples were immediately extracted with dichloromethane following the quenching of reactions. These extracts were then stored at 4 °C to prevent evaporation under atmospheric pressure before analysis using a high resolution gas chromatography-mass spectrometer (SHIMADZU QP2010).

3. Results and discussion

3.1. Activation of PMS

PMS ($2KHSO_5{\cdot}KHSO_4{\cdot}K_2SO_4$) is commonly abbreviated as $HOOSO_3^-$, and is thought to be a mono-SO_3^- substituted hydrogen peroxide (HOOH) [20]. Unlike the symmetrical structures of H_2O_2 and persulfate ($S_2O_8^{2-}$), PMS is an unsymmetrical peroxide. It can contribute one sulfate radical anion ($SO_4^{\bullet -}$) and a hydroxyl radical ($^{\bullet}OH$) by the activation of UV light induction and thereby progress the potential of both $S_2O_8^{2-}$ and H_2O_2 as shown below [11,14,21,22]. The decomposition of PMS in aqueous solution is an important step to yield $SO_4^{\bullet -}$ and $^{\bullet}OH$ (Eq. (3), $E^0 = 1.82$ V) for strong oxidation [17,23], and such $SO_4^{\bullet -}$ can also react with water to yield more hydroxyl radicals [18,22] (Eq. (4)). Although, the reaction rate constant is very low ($k < 60\ M^{-1}\ s^{-1}$), such that the reaction is not a major sink for sulfate radicals; however, the $SO_4^{\bullet -}$ has high efficacy on organic matter:

$$H_2O_2 \xrightarrow{h\nu/\Delta} 2HO^{\bullet} \qquad E^0 = 1.76\ eV \tag{1}$$

$$S_2O_8^{2-} \xrightarrow{h\nu/\Delta} 2SO_4^{\bullet -} \qquad E^0 = 2.12\ eV \tag{2}$$

$$HSO_5^- \xrightarrow{h\nu/\Delta} SO_4^{\bullet -} + HO^{\bullet} \qquad E^0 = 1.82\ eV \tag{3}$$

$$SO_4^{\bullet -} + H_2O \rightarrow H^+ + SO_4^{2-} + HO^{\bullet} \qquad E^0 = 2.60\ eV \tag{4}$$

Thermal induction, in addition to a UV source (λ = 254 nm or λ = 365 nm) can promote the generation of radical species through the photolysis of the oxidants according to Eq. (3) [14,21,22]. Many transition metals, especially divalent metals (Mn^{2+}) which are commonly seen and are important in soil and groundwater systems, also act as electron donors to catalyze the decomposition of PMS through a one-electron transfer reaction analogous to the Fenton initiation reaction. The formation of the sulfate radical in this like-Fenton process, Co^{2+}/PMS, has been recently explored [14,24]:

$$Co^{2+} + HSO_5^- \rightarrow Co^{3+} + (SO_4^{\bullet -} + HO^-) \text{ or } (SO_4^{2-} + HO^{\bullet}) \tag{5}$$

$$Co^{2+} + SO_4^{\bullet -} \rightarrow SO_4^{2-} + Co^{3+} \tag{6}$$

Fig. 2 shows the comparative study (pH, $[BPA]/[BPA]_0$, SO_4^{2-} generation) of the Co^{2+}/PMS oxidation process including varying the amount of the activator (Co^{2+}) and the oxidant (PMS). In comparison to single UV/$S_2O_8^{2-}$ processes (i.e. 1st-stage) [11], the single use of the Co^{2+}/PMS process can not only reach the efficacy of total decomposition of BPA even when buffered at pH 7, but demonstrates a much more efficient mineralization (i.e. detoxication of BPA). Consequently, a much higher TOC removal can be found in Table 1, corresponding to the tendency of BPA degradation displayed in Fig. 2b. This is due to the more powerful $^{\bullet}OH$ donated by Eq. (3) or Eq. (5), instead of the half amount of $SO_4^{\bullet -}$ produced by Eq. (2). This suggests complex chain oxidative processes of events during BPA oxidation by the Co^{2+}/PMS reagent as is stated and further discussed in Eqs. (8)–(21). Table 1 shows that the mineralization was slow after quickly reaching ~40% of the TOC removal. A much longer period of contact or conjunction with other treatments would be needed for total conversion of TOC to CO_2. Recently, some studies also proposed various phenolic compounds such as 2,4-Dichlorophenol (2,4-DCP) can be decayed using a Co^{2+}/PMS process [24,25], but a much higher dosage of PMS/organics mole ratio was applied. As com-

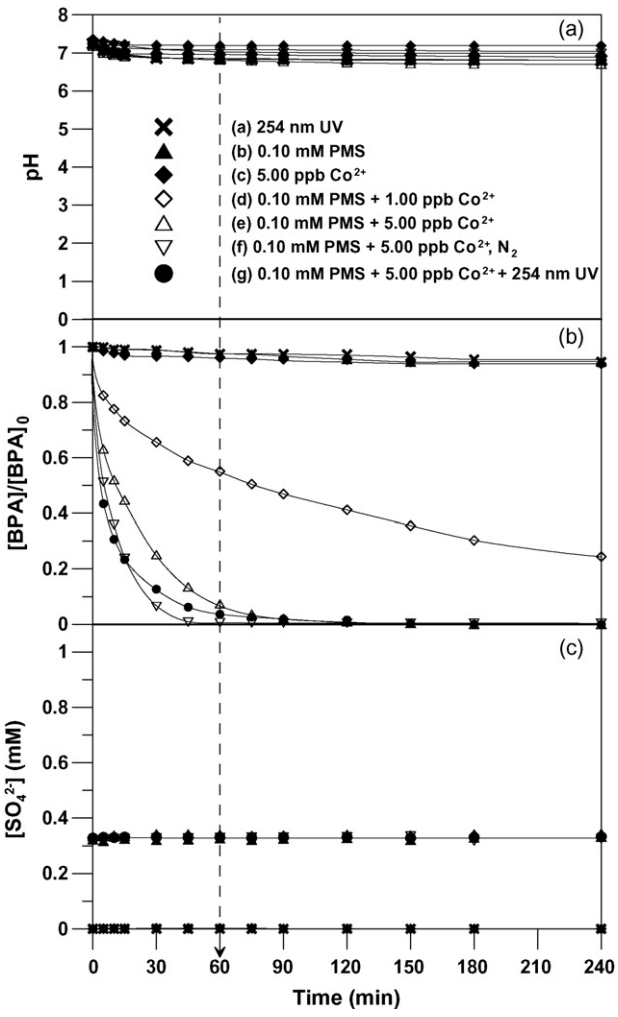

Fig. 2. The pH variations of various oxidation processes in phosphate-buffered solutions (a). BPA degradation during various oxidation processes (b); and the sulfate-ions generation during various oxidation processes (c). The various oxidation processes show the presence of 254 nm UV irradiation only (a); 0.10 mM PMS only (b); 5.00 ppb Co^{2+} only (c); 0.10 mM PMS + 1.00 ppb Co^{2+} (d); 0.10 mM PMS + 5.00 ppb Co^{2+} (e); 0.10 mM PMS + 5.00 ppb Co^{2+}, aeration with N_2 (f); and 0.10 mM PMS + 5.00 ppb Co^{2+} + 254 nm UV (g). $[BPA]_i = 0.05$ mM. Reaction temperature = 25 °C.

Table 1
Comparison of TOC removals among various oxidative processes of 0.05 mM BPA in phosphate-buffered solutions (pH 7) as a function of temperature.

Oxidative processes with different conditions:				[Co(II)] (10^{-4} mM)[a]	[PMS] (mM)	TOC removal (%)						
Run	Temperature (K)	UV				Reaction (min)						
		λ = 254 nm	λ = 365 nm			0	15	30	60	90	120	240
1	298			1.7	0.10	0	9	12	14	14	16	17
2	308			1.7	0.10	0	14	26	27	28	28	29
3	318			1.7	0.10	0	24	29	35	35	35	36
4	298			8.5	0.05	0	11	18	19	26	27	29
5	308			8.5	0.05	0	15	30	33	35	35	38
6	318			8.5	0.05	0	33	34	37	39	39	42
7	298			8.5	0.10	0	22	32	36	37	37	38
8	298	√		8.5	0.10	0	25	37	41	41	41	45
9	298		√	8.5	0.10	0	29	42	47	48	48	49
10	308			8.5	0.10	0	26	36	37	41	41	43
11	318			8.5	0.10	0	28	38	42	42	42	44
12	298			17	0.10	0	24	34	38	38	39	40
13	308			17	0.10	0	27	38	40	40	42	42
14	318			17	0.10	0	28	40	42	43	43	44

[a] 1.7×10^{-4} mM ≃ 1 ppb; 8.5×10^{-4} mM ≃ 5 ppb; 17×10^{-4} mM ≃ 10 ppb.

pared the results in this study (Fig. 2b) with that in previous study [25] by the use of both $CoSO_4$ as the same Co^{2+}-activator source. Neither a high concentration (3.07 mM) nor a low concentration (0.307 mM) of 2,4-DCP with much higher dosages of oxidant (PMS/2,4-DCP = 3–30) and activator (Co^{2+}/PMS = 0.01–0.019) can perform a superior removal efficiency than this work (PMS/BPA = 2; Co^{2+}/PMS = 1.7×10^{-5}–17×10^{-5}) despite 2,4-DCP is a less complex phenolic compound than BPA. This is probably due to $SO_4^{\bullet -}$ (or $SO_3^{\bullet -}$) is a well-known organics-selective radical [26,27] preferred to attack BPA than 2,4-DCP in the beginning of Co^{2+}/PMS processes which is very distinct from the non-selectivity of •OH; and the liberated Cl^- from 2,4-DCP is the most common seen scavenger of free radicals. However, reaching a complete mineralization is not the major objective of this study. Destroying the molecular structure of BPA so as to lower its toxicity was anticipated in order to assess the biodegradability or fate of BPA as it relates to other follow-up biodegradation technologies and to the natural environment. In contrast to UV/$S_2O_8^{2-}$ processes [11], the determined SO_4^{2-} content (~0.15 mM or ~0.30 mM) in the dark reaction solution corresponded to the sulfate content ($KHSO_4 \times K_2SO_4$) of stoichiometry of PMS (0.05 mM or 0.10 mM), and this was almost the initial value for the sulfate-ions at the start of the reaction. However, besides the background value from a $CoSO_4$ source and an acid source for the purpose of adjusting the pH or stabilizing the stock solutions, there was no more specific SO_4^{2-} generated in the solution during the BPA oxidation process (Fig. 2c), indicating that HSO_5^- is not responsible for SO_4^{2-} production.

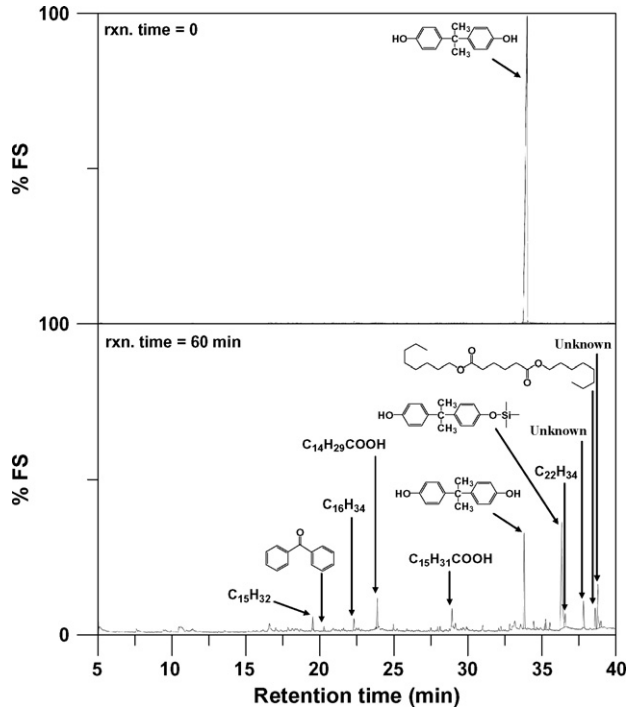

Fig. 3. GC spectra from GC–MS identification of the BPA degradation products formed in the Co^{2+}/PMS oxidation process and are present with retention time. $[BPA]_i$ = 0.05 mM. Reaction temperature = 25 °C.

3.2. BPA degradation and intermediates vicissitude

The GC–MS results of the catalytic-oxidation intermediates for the Co^{2+}/PMS/BPA system are presented in Fig. 3. The results of gas chromatography in Fig. 3 show the 11 obviously different peaks appeared. Among the intermediates, Pentadecane (19.52 min), Benzophenone (20.28 min), Hexadecane (22.32 min), Pentadecanoic acid (23.91 min), Hexadecanoic acid (28.95 min), 2,2-Bis(4-hydroxyphenyl)propane monotrimethylsilyl ether (36.38 min), Docosane (36.61 min), and Hexanedioic acid, dioctyl ester (38.66 min), were identified. Based on the high performance with regard to identification from the GC–MS data base (all have an SI value > 94), these products of mainly long-chain alkanes and carboxylic acids are all biodegradable (i.e. have a much lower toxicity than BPA itself). The possible pathways are further discussed and suggested below in Section 3.4. It should be emphasized that O_2 can always promote the oxidation of organic targets [11,28]. It may contrarily play the role as an inhibitor of radicals during "radical synthesis" process [15] which is verified by a comparison of the results shown in Fig. 2b curves (e) and (f). No obvious signals of the products were observed during the photodegradation of BPA in the absence of PMS (curve (a) of Fig. 2b).

To try to find out the possible interaction of the Co^{2+}/PMS mixture on the promotion of BPA degradation, depth profiles of BPA degradation using UV photo-diode array detection were carried out (Fig. 4). Since BPA is not naturally UV–vis like developed dyes, samples were about 33-multiple concentrated under the same conditions as all of the experimental trials in order to get relatively detectable absorbance spectra with the UV–vis spectrophotometer. The decline of Co(II) species influenced by PMS was evaluated spectrophotometrically at λ = 220–550 nm as a background experiment (Fig. 4a and b). In the present work (Fig. 4c and d), all BPA samples in the oxidation processes, deducting a background value

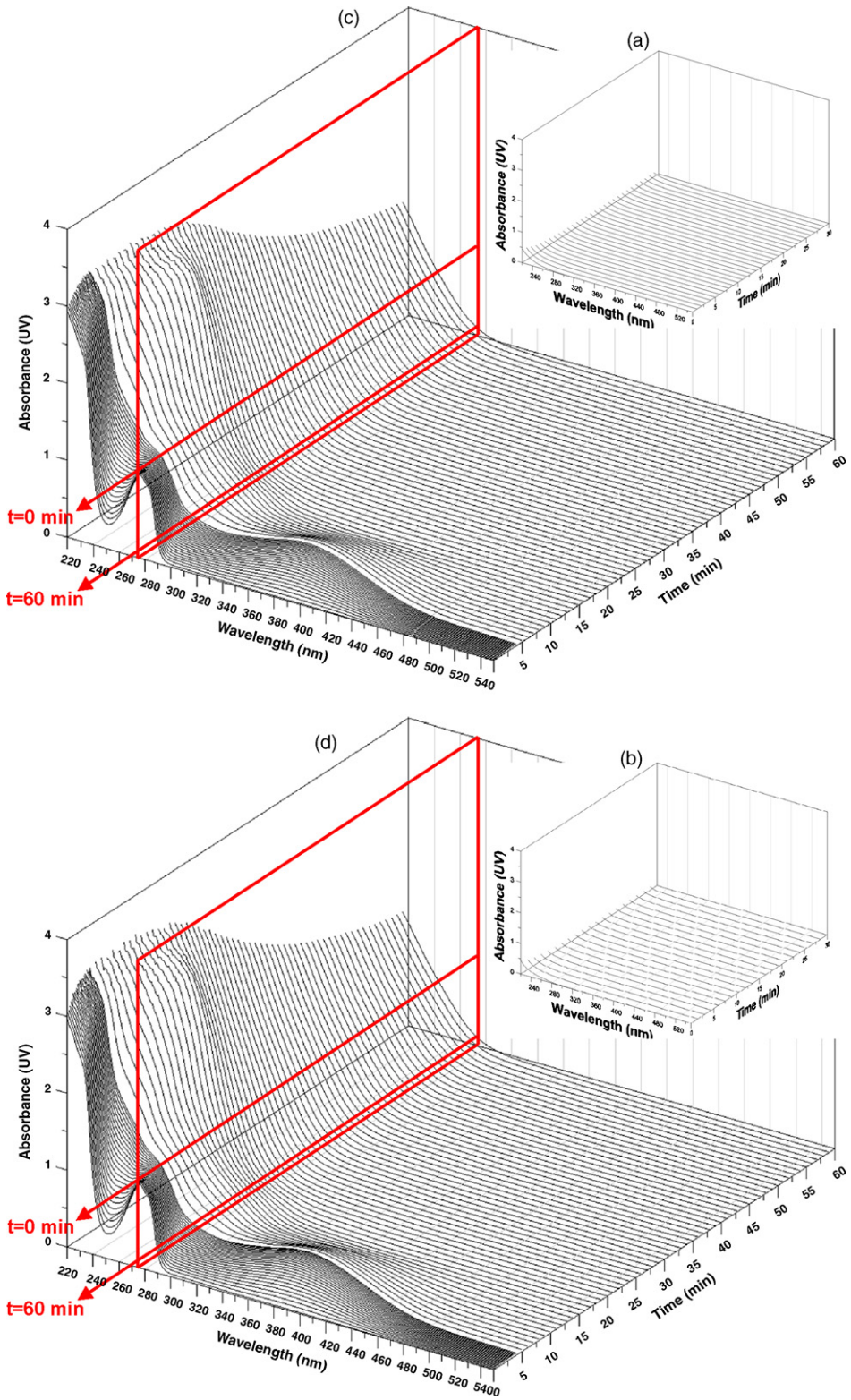

Fig. 4. Absorption UV–vis spectra of unbuffered Co^{2+}/PMS mixture (a); and buffered Co^{2+}/PMS mixture (b) as background experiments, and the absorption UV–vis spectra of BPA and its derivatives in unbuffered Co^{2+}/PMS process (c); or in buffered Co^{2+}/PMS process (d) as comparative study. Reaction temperature = 25 °C.

from Fig. 4a and b, were analyzed immediately after sampling to prevent further reactions.

Fig. 4c shows almost the same profile of BPA with Fig. 4d, verifying no "ion effect" occurred in the presence of PO_4^{3-} in this study. This is not only due to the different organics-selectivity of $SO_4^{\bullet-}$ (or $SO_3^{\bullet-}$) suggested in Section 3.1 but also in the fact that the concentration of PO_4^{3-} (~0.92 mM) used in this buffered process of BPA is much lower than that (0.10 M) in other study [25].

The spectrum at λ = 276 nm is the main absorption wavelength of BPA. Both the absorptions at λ = 254 nm and 300 nm rise to the highest intensities at 12 min and then fall, which relates to the intermediates such as benzoic or phenolic derivatives. Simi-

lar phenomenon of aromatic fragment vicissitude has also been well supported and concluded in many aromatic ring systems in lower UV region [29,30]. These intermediates still remained few after 60 min even though most of the BPA was degraded (>90%), corresponding to the tendency of the finite removal of TOC present in this study.

3.3. Behavior evidence of the dominant radicals

EPR has been mainly used for detection of radical species involved in polymerization, degradation and oxidation. The identification of active radicals involved in this study from the (photo)degradation of BPA with PMS as the oxidant and Co^{2+} as the catalyst was obtained by EPR [21] using a spin-trapping agent, DMPO [31], to yield an EPR detectable product. In order to avoid excessive reactions, the reaction temperature was chosen at 25 °C for EPR analysis though a higher temperature can promote a positive effect on PMS activation (and/or BPA oxidation). But contrarily an incomparable data was present due to the too fast reaction of radicals at heated processes, making the EPR information meaningless. Furthermore, room temperature is always the most feasible consideration of all practical applications include this Co^{2+}/PMS oxidative technology. Certainly, the experiment condition of EPR analysis in Fig. 5 has a correspondence with curve (e) and (f) in Fig. 2. After treatment with DMPO at 25 °C, the EPR spectra of Co(II) + PMS, Co(II) + PMS + BPA, photon + Co(II) + PMS, and photon + Co(II) + PMS + BPA at different pH value are shown in the Fig. 5. Comparing the spectrum of Fig. 5c and d with Fig. 5a and b, the characteristic peak of the •OH radical is much more obvious in Fig. 5c and d than it is in Fig. 5a and b due to the photolysis of PMS (Eq. (3)) and the side reaction (Eq. (7)) when using the UV source as an additional activator, especially at acidic or basic conditions (i.e. pH 5 or pH 11).

$$SO_4^{\bullet-} + H_2O \xrightarrow{h\nu} SO_4^{2-} + {}^{\bullet}OH + H^+ \quad (7)$$

This is quite different from the persulfate system described in our previous study [11] in which there was no obvious characteristic $SO_4^{\bullet-}$ peak found in the dark Co^{2+}/PMS process. However, a similar result in acidic conditions (pH 5) can be found, where a particular number of characteristic peaks are proposed to be $SO_3^{\bullet-}$ spectrum in the UV/Co^{2+}/PMS process. The $SO_3^{\bullet-}$ spectrum is authentically identified from the intensity ratio of 4 characteristic peaks as 1:1:1:1 [32], which is qualitatively different to the 3 peaks (i.e. 1:1:1) of the $SO_4^{\bullet-}$ spectrum [31]. The $SO_3^{\bullet-}$ spectrum is indicated by the series of symbols as "①:①:①:①" in Fig. 5. This is because of the fact that the hydrolysis equilibrium of HSO_5^- take place (Eq. (10)) [33,34], leading to the subsequent chain oxidative reactions involving $SO_3^{\bullet-}$ generation (Eqs. (11)–(13)). Furthermore, the •OH spectrum is identified to be the dominator, not only in the dark Co^{2+}/PMS process, but also in the UV/Co^{2+}/PMS process, as a result of the intensity ratio of each characteristic peak being 1:2:2:1 [35], which overlapped the $SO_3^{\bullet-}$ spectrum indicates the participation of $SO_3^{\bullet-}$ and •OH coexistently in the BPA degradation. The •OH spectrum is indicated by the series of symbols as "❶:❷:❷:❶" in Fig. 5. It is very interesting that the $SO_4^{\bullet-}$ produced (Eq. (5)) seems to be more unstable in the Co^{2+}/PMS process, preferring to transform into •OH rapidly at any pH. Even in the UV/Co^{2+}/PMS process, the •OH spectrum is still more obvious than that of the $SO_3^{\bullet-}$ spectrum at acidic conditions (pH 5), indicating that it is the dominator. Contrary to the Co^{2+}/PMS process, $SO_4^{\bullet-}$ is rather stable in the acidic persulfate process (pH ≤ 5); and •OH becomes the dominator only when the solution pH is greater than 10.7 [11,21]. To the best of our knowledge, the point of view proposed above is the first attempt to show that the dominant behavior of radicals in a (bi)sulfite process is very different from that in a persulfate process.

Furthermore, another meaningful proof is proposed through the comparison of the spectra of Fig. 5a and c with those in Fig. 5b and d. The relatively strong spectra only observed at pH ≥ 7 (especially at pH 7) with an intensity ratio of characteristic peaks being 1:2:1:2:1:2:1 are identified to be the corresponding nitroxide radical (5,5-dimethylpyrrolidone-(2)-oxyl-(1); DMPOX) of DMPO [36] even is present as over-scale large as shown in the UV/Co^{2+}/PMS process (curve (b) of Fig. 5c). The DMPO spectrum is indicated by the series of symbols as "(1):(2):(1):(2):(1):(2):(1)" in Fig. 5. It should be especially noticed that a nitroxide radical such as DMPOX detected in these incubation processes did not result from spin-trapping (i.e. not a DMPO-HO• adduct), but rather from direct oxidation by a variety of single electron sources as shown in the study of Floyd and Soong (1977) [37]. This is because of an immense amount of •OH suddenly generated at pH 7 and corresponding to the produced H_2O_2 as an additional •OH source resulting from the hydrolysis of HSO_5^- under neutral conditions (Eq. (10)) [33,34], indicating that most of the spin-trapping agent oxidized to DMPOX in the absence of target organic, BPA. On the contrary, little or no intensities of DMPOX spectra can be observed in Fig. 5b and d due to the participation of BPA as a preferred compound reacting to •OH rather than to DMPO. The reasonable spectrum is shown corresponsively in curve (b) of Fig. 5d, the extra species of •OH having survived after reacting with BPA but then spin-trapped by DMPO and present as DMPO-HO• adducts, or it may be present as a DMPOX spectrum again as shown in curve (b) of Fig. 5b while sufficient detectable numbers of survival (•OH) for direct oxidation of DMPO in the same analysis time. Therefore, the above performances having only occurred at neutral pH indicates that solutions with extreme acidic or basic conditions do not provide the best conditions for efficient organic degradation (oxidation) by PMS. Organic molecules are more rapidly oxidized by the PMS process in neutral pH than in pure water. This conclusion has been previously suggested [38] and is coincidentally similar to that of a persulfate system [11,39], but has never been directly evidenced in detail as has been done in this study.

3.4. Possible chain oxidative pathways of BPA

In contrast to another study [40] but similar to our previous research [11], the results from our control experiments indicate that thermal effects did take place between the metal-ions (i.e. Co^{2+}) and the PMS, and this was observed especially between PMS and BPA (Table 1). The metal-ions used throughout this work do not absorb the UV radiation in the visible region (300–760 nm) as is the case when coabsorbed with PMS at wavelengths below 300 nm (Fig. 4). Hence, the main absorbing species is the BPA.

On the basis of the above experimental results and literature information [40,41], the contribution of Co^{2+} as a catalyst and PMS as an oxidant to the BPA degradation suggested in this section is deduced from incorporating the evidence found in Figs. 2–5. Hence, it was verified that no reactive intermediate is formed directly through the thermal reaction between Co^{2+} and PMS or Co^{2+} and BPA. The possible chain oxidative pathways for the degradation of BPA with Co^{2+} and PMS under thermal promotion or UV irradiation are suggested below in Eqs. (8)–(17) in order to describe the mineralization mechanism of BPA:

$$BPA + Co^{2+} \rightarrow [BPA\cdots Co^{2+}] \quad (8)$$

$$[BPA\cdots Co^{2+}] \xrightarrow{h\nu/\Delta} [BPA\cdots Co^{2+}]^* \quad (9)$$

The hydrolysis equilibrium [33,34] of HSO_5^- is also reported to take place in neutral conditions [42] as represented by Eq. (10) as follows:

$$HSO_5^- + H_2O \leftrightarrow H_2O_2 + HSO_4^- \quad (10)$$

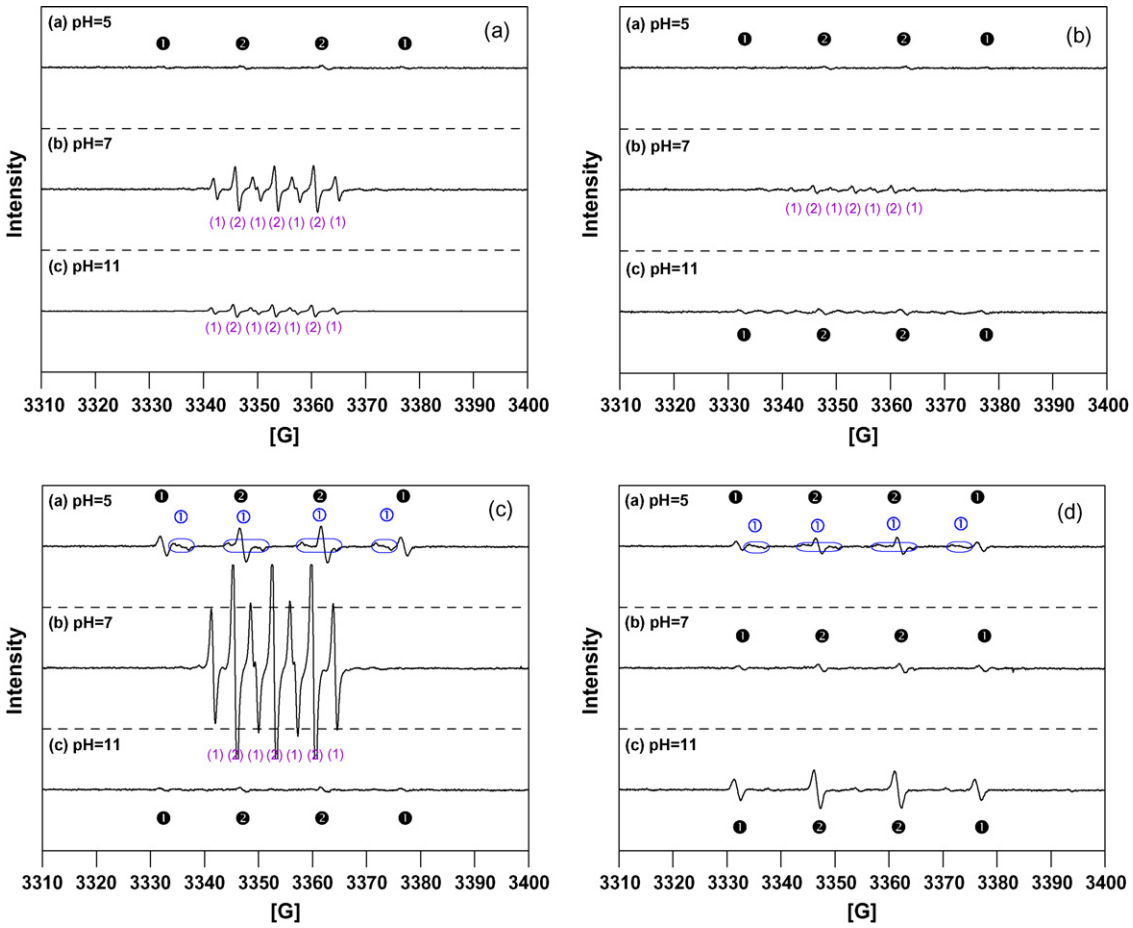

Fig. 5. EPR spetra of Co(II) + PMS (a), Co(II) + PMS + BPA (b), photon + Co(II) + PMS (c), and photon + Co(II) + PMS + BPA (d) at different pH value (acidic or neutral or alkaline). Each trial of 0.10 mM PMS solution with 5.00 ppb Co^{2+} was, or was not, photo-activated within 10 min of illumination, and was thus detected by EPR with the participation of BPA to identify the expected $SO_4^{\bullet-}$ or $SO_3^{\bullet-}$ or $^{\bullet}OH$ produced. Center field = 3355 G, sweep width = 100 G, microwave frequency = 9.4 GHz, and power setting = 20 mW. All spectra intensities are present in the same scale of *Y*-axis (−14000 to 14000). Operating temperature = 25 °C.

$$[BPA\cdots Co^{2+}]^* + HSO_5^- \text{ or } HSO_4^- \rightarrow BPA^{\bullet+} + Co^{2+} + (HO^- + SO_4^{\bullet-} \text{ or } SO_3^{\bullet-}) \quad (11)$$

$$BPA^* + HSO_5^- \text{ or } HSO_4^- \rightarrow BPA^{\bullet+} + (HO^- + SO_4^{\bullet-} \text{ or } SO_3^{\bullet-}) \quad (12)$$

$$BPA^{\bullet+} + HSO_5^- \text{ or } HSO_4^- \rightarrow [\text{organics (HR)}] + (HO^- + SO_4^{\bullet-} \text{ or } SO_3^{\bullet-}) \quad (13)$$

$$Co^{2+} + HSO_5^- \text{ or } HSO_4^- \rightarrow Co^{3+} + (HO^- + SO_4^{\bullet-} \text{ or } SO_3^{\bullet-}) \text{ or } (HO^{\bullet} + SO_4^{2\bullet-} \text{ or } SO_3^{2-}) \quad (14)$$

$$BPA^{\bullet+} + Co^{2+} \text{ or } Co^{3+} \rightarrow \text{organics} + Co^{2+} \text{ or } Co^{3+} \quad (15)$$

$$\text{Organic} + HO^{\bullet} + SO_4^{\bullet-} \text{ or } SO_3^{\bullet-} \rightarrow [\text{radicalintermediates}(R^{\bullet})] \quad (16)$$

The metal-catalyzed autoxidation of the (bi)sulfite anion, studied for decades, is also proposed to be an oxygen-consuming chain reaction [22,28,32], including:

$$R^{\bullet} + (HSO_5^- \text{ or } HSO_4^-)/O_2 \rightarrow \text{organics} \rightarrow CO_2 + H_2O \quad (17)$$

The possible side reactions and the Co^{2+} (i.e. divalent metals) regeneration [9,14,24] are suggested below, thereby progress the efficient activation of PMS and degradation of BPA continuously even with an extremely low $[Co^{2+}]_0 = 5\ \mu g\ L^{-1}$:

$$HSO_5^- \text{ or } HSO_4^- + (SO_4^{\bullet-} \text{ or } SO_3^{\bullet-} \text{ or } HO^{\bullet}) \rightarrow SO_5^{\bullet-} \text{ or } SO_4^{\bullet-} + (SO_4^{2-} \text{ or } SO_3^{2-} \text{ or } HO^-) + H^+ \quad (18)$$

$$Co^{3+} + HSO_5^- \text{ or } HSO_4^- \rightarrow Co^{2+} + SO_5^{\bullet-} \text{ or } SO_4^{\bullet-} + H^+ \quad (19)$$

$$R^{\bullet} + O_2 \rightarrow ROO^{\bullet} \xrightarrow{Co^{3+}} \text{oxygenated products} \rightarrow Co^{2+} + {}^{\bullet}OH \quad (20)$$

The dissolved O_2 seems to play an active role leading to the peroxy-radicals, $ROO^{\bullet}$ (R = H, alkyl, aryl) [43,44], and $ROO^{\bullet}$ will serve as chain propagators and oxidize organic materials either by hydrogen abstraction or by an electron transfer process [45,46]. There is even a high opportunity for it to collide with another radical intermediate ($R^{\bullet}$ or $ROO^{\bullet}$) to yield a macromolecule [15] as well as partial polymerization as shown in Fig. 3:

$$ROO^{\bullet} \text{ or } R^{\bullet} + (ROO^{\bullet} \text{ or } R^{\bullet}) \rightarrow \text{macromolecularorganics} \quad (21)$$

3.5. Kinetics approach

The decomposition of PMS in aqueous solution is an important step in producing powerful radicals ($SO_4^{\bullet-}$ or $SO_3^{\bullet-}$ or $^{\bullet}OH$) which destroy organic compounds such as BPA; however, temperature is the critical factor influencing the decomposition of PMS (data pre-

Table 2
Kinetic rate constants of Co(II)-activated PMS oxidation of 0.05 mM BPA in phosphate-buffered solutions (pH 7) as a function of temperature.

Run	[Co(II)] (10^{-4} mM)	[PMS] (mM)	Temperature (K)	Initial rate (mM min^{-1})[a]	BPA decay of R_i (%)[b]	k_{obs} (min^{-1})[c]	R^2 of k_{obs}	$t_{1/2}$ (min)[d]	ΔE (kJ mol^{-1})	R^2 of ΔE
1	1.7	0.10	298	1.6×10^{-3}	17	1.1×10^{-2}	0.72	75	77.96	0.98
2	1.7	0.10	308	3.0×10^{-3}	31	4.2×10^{-2}	0.95	15		
3	1.7	0.10	318	3.6×10^{-3}	37	8.4×10^{-2}	0.99	8		
4	8.5	0.05	298	3.2×10^{-3}	34	4.2×10^{-2}	0.85	13	52.16	0.95
5	8.5	0.05	308	4.8×10^{-3}	49	11.1×10^{-2}	0.97	5		
6	8.5	0.05	318	4.8×10^{-3}	51	15.9×10^{-2}	0.99	4		
7	8.5	0.10	298	3.6×10^{-3}	37	4.7×10^{-2}	0.95	11	57.62	0.94
8	8.5	0.10	308	4.9×10^{-3}	52	13.7×10^{-2}	0.99	4		
9	8.5	0.10	318	6.1×10^{-3}	57	20.3×10^{-2}	0.98	4		
10	17	0.10	298	3.5×10^{-3}	38	7.6×10^{-2}	0.99	8	61.57	0.99
11	17	0.10	308	6.3×10^{-3}	65	18.8×10^{-2}	0.99	3		
12	17	0.10	318	7.2×10^{-3}	76	36.3×10^{-2}	0.98	3		

[a] The initial rate was expressed by the decreased BPA concentration (ΔC) per minute (within first 5 min).
[b] R_i indicates the initial rate at first 5 min.
[c] k_{obs} (observed rate constant): The pseudo-first-order kinetics constant for the oxidation of BPA by Co/PMS.
[d] Half-life time of BPA in Co/PMS oxidation process.

sented in Table 1). Based on this, the effects of temperature and the activation energy of our BPA degradation system were studied. Table 2 shows the influence of temperature and Co^{2+} dosage on the PMS oxidation of BPA over a range of 25–45 °C. BPA degradation rates can be improved under thermally enhanced conditions, resulting in the degradation of BPA after 5 min being ~37% at 25 °C, ~52% at 35 °C, and ~57% at 45 °C, respectively, shown in runs 7–9. All BPA degradations can reach an expected value >90% after 1 h, corresponding with the respective TOC removal data shown in Table 1.

Accordingly, it was found in this Co^{2+}/PMS/BPA process that the BPA degradation is well formulated to the pseudo-first-order kinetics. There is a very good fit of all the experimental data to a pseudo-first-order model, using the exponential regression analysis (data presented in Table 2) formulated from the original plot of the normalized remaining concentration ($[BPA]/[BPA]_0$) vs. reaction time (t). The pseudo-first-order rate constants (k_{obs}) of BPA degradation were found to be 0.047 min^{-1} ($R^2 = 0.95$) at 25 °C, 0.137 min^{-1} ($R^2 = 0.99$) at 35 °C, and 0.203 min^{-1} ($R^2 = 0.98$) at 45 °C, respectively, as shown in runs 7–9, along with an increase with increased temperatures. Temperature effect in this study is more obvious than that of a UV/persulfate system [11].

In comparison to a UV/persulfate system, the activation energy ($\Delta E = 57.6$ kJ mol^{-1}) in this dark Co^{2+}/PMS system is estimated easily from the Arrhenius plot but is twice as high as that in our previous study [11]. This may be due to the various reactivities with target organics between the selected inorganic radicals (E^0 of $SO_4^{\bullet-} = 2.60$ V; E^0 of $SO_5^{\bullet-} = 1.1$ V) [24] and also to the absence of the shrinkage of the reaction energy barrier (Eq. (2)) by extra activation from a UV source (254 nm). Furthermore, comparing runs 4–6 with runs 7–9 in Table 2, it can be seen that the activity of BPA degradation is not obviously dependent on the PMS concentration, but rather is related to the Co^{2+} dosage as contrasted with a comparison of runs 1–3 with runs 7–9 (or runs 10–12). The results of the activation energy also suggest that the optimum dosage of Co^{2+} catalyst is sufficient at 8.5×10^{-4} mM (i.e. 5 ppb) for activation of 0.10 mM PMS in a dark reaction process.

4. Conclusions

Only a molar ratio of $[PMS]_0/[BPA]_0 = 2$ and a minimum dosage of $[Co^{2+}]_0 = 5$ ppb are successfully utilized in pH 7 for more efficient detoxication (~40% mineralization at 1 h) of BPA during the dark Co^{2+}/PMS process instead of the 1st-stage oxidation in the UV-$Na_2S_2O_8/H_2O_2$-Fe(II,III) process observed in our previous work. The 40% of TOC removal is much superior to that of almost no mineralization in our previous study, thereby, the substitutive technology of Co^{2+}/PMS process can meet the requirements of oxidizing BPA to less complex compounds more efficient within 1 h as the 1st-stage. Hence the proposed procedure has great potential for lowering operational costs and can be practically implemented with other AOPs or industrial biological processes. As the successful results show, the possibility of any involvement of $^{\bullet}OH$ and $SO_3^{\bullet-}$ free radicals has been eliminated, and the dominant behavior of radicals have also been evidenced in the first attempt. Activation parameters such as the rate constant and the energy of activation have been well formulated by the pseudo-first-order reaction rate, and the possible reaction pathways based on the identification of radicals and intermediates with an extremely low concentration of Co^{2+} are demonstrably suggested.

Acknowledgement

The authors would like to thank the National Science Council of the Republic of China, Taiwan, for financially supporting this research under Contract No. NSC 97-2221-E-006-042.

References

[1] C.A. Staples, P.B. Dorn, G.M. Klecka, S.T. O'Block, L.R. Harris, A review of the environmental fate, effects, and exposures of Bisphenol A, Chemosphere 36 (1998) 2149–2173.
[2] C.A. Staples, P.B. Dorn, G.M. Klecka, S.T. O'Block, D.R. Branson, L.R. Harris, Bisphenol A concentrations in receiving waters near US manufacturing and processing facilities, Chemosphere 40 (2000) 521–525.
[3] T.E. Schafer, C.A. Lapp, C.M. Hanes, J.B. Lewis, J.C. Wataha, G.S. Schuster, Estrogenicity of bisphenol A and bisphenol A dimethacrylate in vitro, J. Biomed. Mater. Res. 45 (1999) 192–197.
[4] J.H. Kang, F. Kondo, Bisphenol A degradation by bacteria isolated from river water, Arch. Environ. Contam. Toxicol. 43 (2002) 264–269.
[5] C. Zhang, G. Zeng, L. Yuan, J. Yu, J. Li, G. Huang, B. Xi, H. Liu, Aerobic degradation of bisphenol A by Achromobacter xylosoxidans strain B-16 isolated from compost leachate of municipal solid waste, Chemosphere 68 (2007) 181–190.
[6] N. Watanabe, S. Horikoshi, H. Kawabe, Y. Sugie, J. Zhao, H. Hidaka, Photodegradation mechanism for bisphenol A at the TiO_2/H_2O interfaces, Chemosphere 52 (2003) 851–859.
[7] D. Zhou, F. Wu, N. Deng, W. Xiang, Photooxidation of bisphenol A (BPA) in water in the presence of ferric and carboxylate salts, Water Res. 38 (2004) 4107–4116.
[8] Y.H. Huang, Y.F. Huang, P.S. Chang, C.Y. Chen, Comparative study of oxidation of dye-Reactive Black B by different advanced oxidation processes: Fenton, electro-Fenton and photo-Fenton, J. Hazard. Mater. 154 (2008) 655–662.
[9] Y.H. Huang, S.T. Tsai, Y.F. Huang, C.Y. Chen, Degradation of commercial azo dye reactive Black B in photo/ferrioxalate system, J. Hazard. Mater. 140 (2007) 382–388.
[10] S. Tanaka, M. Kawai, Y. Nakata, M. Terashima, H. Kuramitz, M. Fukushima, Degradation of bisphenol A by photo-fenton processes, Toxicol. Environ. Chem. 85 (2003) 95–102.

[11] Y.F. Huang, Y.H. Huang, Identification of produced powerful radicals involved in the mineralization of Bisphenol A using a novel UV-$Na_2S_2O_8$/H_2O_2-Fe(II,III) two-stage oxidation process, J. Hazard. Mater. 162 (2009) 1211–1216.
[12] T. Pandurengan, P. Maruthamuthu, Kinetics and mechanism of oxidation of dimethyl sulfoxide by peroxomonosulfate, B. Chem. Soc. Jpn. 54 (1981) 3551–3555.
[13] R. Renganathan, P. Maruthamuthu, Kinetics and mechanism of oxidation of aliphatic aldehydes by peroxomonosulphate, Int. J. Chem. Kinet. 18 (1986) 49–58.
[14] G.P. Anipsitakis, D.D. Dionysiou, Transition metal/UV-based advanced oxidation technologies for water decontamination, Appl. Catal. B-Environ. 54 (2004) 155–163.
[15] G. Manivannan, P. Maruthamuthu, Peroxo salts as initiators of vinyl polymerization-III. Polymerization of acrylonitrile initiated by the peroxomonosulphate-Co(II) redox system, Eur. Polym. J. 23 (1987) 311–313.
[16] K.C. Huang, Z.q. Zhao, G.E. Hoag, A. Dahmani, P.A. Block, Degradation of volatile organic compounds with thermally activated persulfate oxidation, Chemosphere 61 (2005) 551–560.
[17] C.J. Liang, I.L. Lee, I.Y. Hsu, C.P. Liang, Y.L. Lin, Persulfate oxidation of trichloroethylene with and without iron activation in porous media, Chemosphere 70 (2008) 426–435.
[18] G.R. Peyton, The free-radical chemistry of persulfate-based total organic carbon analyzers, Mar. Chem. 41 (1993) 91–103.
[19] X.Y. Yu, Z.C. Bao, J.R. Barker, Free radical reactions involving $Cl^{\bullet}$, $Cl_2^{\bullet-}$, and $SO_4^{\bullet-}$ in the 248 nm photolysis of aqueous solutions containing $S_2O_8^{2-}$ and Cl^-, J. Phys. Chem. A 108 (2004) 295–308.
[20] P. Kanakaraj, P. Maruthamuthu, Kinetics and mechanism of photochemical reactions of peroxomonosulfate in the presence and absence of 2-propanol, Int. J. Chem. Kinet. 15 (1983) 1301–1310.
[21] L. Dogliotti, E. Hayon, Flash photolysis of persulfate ions in aqueous solutions. Study of the sulfate and ozonide radical anions, J. Phys. Chem. 71 (1967) 2511–2516.
[22] E. Hayon, A. Treinin, J. Wilf, Electronic spectra, photochemistry, and autoxidation mechanism of the sulfite-bisulfite-pyrosulfite systems. SO_2^-, SO_3^-, SO_4^-, and SO_5^- radicals, J. Am. Chem. Soc. 94 (1972) 47–57.
[23] L. Eberson, Electron Transfer Reactions in Organic Chemistry, Spring-Verlag, Berlin, 1987.
[24] G.P. Anipsitakis, D.D. Dionysiou, Degradation of organic contaminants in water with sulfate radicals generated by the conjunction of peroxymonosulfate with cobalt, Environ. Sci. Technol. 37 (2003) 4790–4797.
[25] G.P. Anipsitakis, D.D. Dionysiou, M.A. Gonzalea, Cobalt-mediated activation of peroxymonosulfate and sulfate radical attack on phenolic compounds. Implications of chloride ions, Environ. Sci. Technol. 40 (2006) 1000–1007.
[26] C. Cuypers, T. Grotenhuis, K.G.J. Nierop, E.M. Franco, A.D. Jager, W. Rulkens, Amorphous and condensed organic matter domains: the effect of persulfate oxidation on the composition of soil/sediment organic matter, Chemosphere 48 (2002) 919–931.
[27] G.H. Scott, E.P. Bruce, In-Situ Chemical Oxidation-Engineering Issue, Ground Water and Ecosystem Restoration Information Center, UAEPA, EPA/600/R-06/072, 2006, http://www.epa.gov/ada/download/issue/600R06072.pdf.
[28] J.M. McCord, I. Fridovich, The utility of superoxide dismutase in studying free radical reactions, J. Biol. Chem. 244 (1969) 6056–6063.
[29] M.S. Lucas, J.A. Peres, Decolorization of the azo dye reactive Black 5 by Fenton and photo-Fenton oxidation, Dyes Pigments 71 (2006) 236–244.
[30] J.H. Sun, S.P. Sun, G.L. Wang, L.P. Qiao, Degradation of azo dye Amido black 10B in aqueous solution by Fenton oxidation process, Dyes Pigments 74 (2007) 647–652.
[31] S.C. Hsu, T.M. Don, W.Y. Chiu, Free radical degradation of chitosan with potassium persulfate, Polym. Degrad. Stabil. 75 (2002) 73–83.
[32] G.A. Reed, J.F. Curtis, C. Mottley, T.E. Eling, R.P. Mason, Epoxidation of (±)-7,8-dihydroxy-7,8-dihydrobenzo[α]pyrene during (bi)sulfite autoxidation: activation of a procarcinogen by a cocarcinogen, Proc. Natl. Acad. Sci. USA 83 (1986) 7499–7502.
[33] D.L. Ball, J.O. Edwards, The kinetics and mechanism of the decomposition of Caro's Acid. I, J. Am. Chem. Soc. 78 (1956) 1125–1129.
[34] S. Dubey, S. Hemkar, C.L. Khandelwal, P.D. Sharma, Kinetics and mechanism of oxidation of hypophosphorous acid by peroxomonosulphate in acid aqueous medium, Inorg. Chem. Commun. 5 (2002) 903–908.
[35] Y. Huang, J. Li, W. Ma, M. Cheng, J. Zhao, J.C. Yu, Efficient H_2O_2 oxidation of organic pollutants catalyzed by supported iron sulfophenylporphyrin under visible light irradiation, J. Phys. Chem. B 108 (2004) 7263–7270.
[36] G.M. Rosen, E.J. Rauckman, Spin trapping of the primary radical involved in the activation of the carcinogen N-hydroxy-2-acetylaminofluorene by cumene hydroperoxide-hematin, Mol. Pharmacol. 17 (1980) 233–238.
[37] R.A. Floyd, L.M. Soong, Spin trapping in biological systems. Oxidation of the spin trap 5,5-dimethyl-1-pyrroline-1-oxide by a hydroperoxide-hematin system, Biochem. Biophys. Res. Commun. 74 (1977) 79–84.
[38] T.C. Zheng, D.E. Richardson, Homogeneous aqueous oxidation of organic molecules by oxone and catalysis by a water-soluble manganese porphyrin complex, Tetrahedron Lett. 36 (1995) 833–836.
[39] P.D. Goulden, D.H.J. Anthony, Kinetics of uncatalyzed peroxydisulfate oxidation of organic material in fresh water, Anal. Chem. 50 (1978) 953–958.
[40] J. Fernandez, P. Maruthamuthu, J. Kiwi, Photobleaching and mineralization of Orange II by oxone and metal-ions involving Fenton-like chemistry under visible light, J. Photochem. Photobiol. A 161 (2004) 185–192.
[41] J. Bandara, J. Kiwi, Fast kinetic spectroscopy, decoloration and production of H_2O_2 induced by visible light in oxygenated solutions of the azo dye Orange II, N. J. Chem. 23 (1999) 717–724.
[42] J. Balej, Thermodynamics of reactions during the electrosynthesis of peroxodisulphates, Electrochim. Acta 29 (1984) 1239–1242.
[43] V. Nadtochenko, J. Kiwi, Photoinduced adduct formation between Orange II and $[Fe^{3+}(aq)]$ or $Fe(ox)_3^{3-}$—H_2O_2 photocatalytic degradation and laser spectroscopy, J. Chem. Soc. Faraday T 93 (1997) 2373–2378.
[44] B. Ruppert, R. Bauer, G. Heisler, The photo-Fenton reaction—an effective photochemical waste-water treatment process, J. Photochem. Photobiol. A 73 (1993) 75–78.
[45] K.U. Ingold, Peroxy radicals, Acc. Chem. Res. 2 (1969) 1–9.
[46] B. Maillard, K.U. Ingold, J.C. Scaiano, Rate constants for the reactions of free radicals with oxygen in solution, J. Am. Chem. Soc. 105 (1983) 5095–5099.